Faceting and structural anisotropy of nanopatterned CdO(110) layers

J. Zúñiga-Pérez,[a] C. Martínez-Tomás, and V. Muñoz-Sanjosé
Departamento de Física Aplicada y Electromagnetismo, Universitat de València, C/Dr. Moliner 50, 46100 Burjassot, Spain

C. Munuera and C. Ocal
Instituto de Ciencia de Materiales de Madrid, Consejo Superior de Investigaciones Científicas, 28049 Cantoblanco, Spain

M. Laügt
Centre de Recherche sur l'Hétéro-Epitaxie et ses Applications, Centre National de la Recherche Scientifique, Rue Bernard Gregory, Parc Sophia Antipolis, F-06560 Valbonne, France

(Received 17 March 2005; accepted 14 June 2005; published online 10 August 2005)

CdO(110) layers with a self-organized surface structure have been grown on $(10\bar{1}0)$ sapphire (*m* plane) substrates by metal-organic vapor phase epitaxy. The epitaxial relationships between layer and substrate have been determined and a crystallographic model that accounts for the CdO in-plane orientation, which results in a reduced lattice mismatch when the CdO[001] direction is perpendicular to the sapphire *c* axis, has been proposed. Although the measured lattice parameters indicate that the layers are almost fully relaxed, an anisotropic mosaicity is detected with symmetrical rocking curves attaining minimum values when measured along the CdO$[\bar{1}10]$ direction. The layer morphology consists of a regular ridge-and-valley structure which defines, again, a preferential in-plane direction. The grooves run parallel to the CdO[001] axis and exhibit lateral surfaces sloped at 28° with respect to the (110) surface. The influence of growth temperature and VI/II molar ratio on the anisotropic mosaicity and morphology has been analyzed. © *2005 American Institute of Physics*. [DOI: 10.1063/1.1997267]

I. INTRODUCTION

Surfaces showing a nanopatterned structure have been used in the last decade in numerous microelectronic, optical, and microelectromechanical applications.[1] In particular, regular ordering of quantum dots[2] and of metallic and magnetic nanoparticles[3–5] has been achieved. Electron-beam lithography and ion etching are the most popular methods for creating these patterned substrates in inorganic materials,[6] although their low throughput makes them useless in large-scale industrial production. One of the simplest approaches to overcome this disadvantage consists of using self-organized facets which develop in materials exhibiting rock salt structure either during the growth process[3–5] or while etching/annealing them. NaCl substrates, etched with water and annealed in vacuum at 450 °C,[7] showed macrosteps running along the [001] direction and presented {100}-type facets which enabled spatial ordering of Fe nanowires[8] and Fe and Au nanoparticles.[3,4] Another rock salt material that has been extensively studied is MgO, an ionic oxide commonly used as substrate or buffer layer for superconducting and ferroelectric materials. Since the report on the faceting of MgO(110) by Henrich,[9] this surface has been investigated both theoretically[10] and experimentally.[5,11–13] Goniakowski and Noguera calculated the surface energy of MgO(110) and several vicinal surfaces and demonstrated that {100}-type MgO surfaces are energetically favorable,[10] confirming the results early obtained by Wolf on NaCl and MgO.[14,15] Thus, surface energy minimization would support faceting of MgO into {100}, as in electron-ion bombarded substrates[9] and homoepitaxially grown layers.[13] Nevertheless several authors have found other facet orientations.[5,11,12] Interestingly, some of the faceted surfaces displayed a self-organized groove structure whose edges ran parallel to either the [001] or $[1\bar{1}0]$ direction, although no reasons for such particular alignments were proposed. It is worth noticing that the groove structure in the [001] direction was obtained by deposition of a MgO layer,[13] while in the second case the structure was obtained by annealing in air a MgO substrate at temperatures above 1273 K.[5]

MgO belongs to the same II/VI oxide family as ZnO and CdO. All three materials have received increasing attention in the last years due to their possibilities in optoelectronic applications working in the blue and ultraviolet wavelength regions.[16] Under standard pressure conditions ZnO crystallizes in a wurtzite structure while CdO does in rock salt,[17] as MgO. Likely, CdO should tend to facet into minimum energy {100} surfaces. In a previous work we studied the growth of CdO(001) layers directly on $(01\bar{1}2)$ sapphire (*r* plane) and found that morphology and crystalline quality strongly depended on growth temperature.[18] However, to study the faceting of CdO is necessary to obtain CdO surfaces other than (100). In this article we report on the growth of rock salt CdO(110) layers on *m*-plane sapphire and investigate their structural and morphological properties by high-resolution x-ray diffraction (HRXRD) and scanning force microscopy (SFM). A systematic study on the influence of growth temperature and VI/II molar ratio on the properties of the layers has been carried out, paying special attention to anisotropic

[a]Electronic mail: jesus.zuniga@uv.es

effects. Additionally, a crystallographic model which accounts for the epitaxial relationships between layer and substrate as well as for the elongation direction of the self-organized groove structure has been proposed.

II. EXPERIMENTAL DETAILS

The CdO samples were grown on *m*-plane sapphire substrates by employing a horizontal two-inlet metal-organic vapor phase epitaxy (MOVPE) reactor operated at atmospheric pressure with nitrogen being used as carrier gas. The cadmium and oxygen precursors, dimethylcadmium (DMCd) and tertiary butanol (*tert*-butanol), were introduced into the reaction chamber through the upper and lower inlets, respectively, so that the complete mixing of both precursors occurred at the beginning of the first substrate wafer.[19] The sapphire substrates, oriented to within ±0.25° of the *m* plane, were used as received without any prior thermal or chemical treatment. In order to study the influence of growth temperature, the graphite susceptor was rf heated to temperatures between 271 and 405 °C while maintaining a constant *tert*-butanol to DMCd flux ratio equal to 10. A second series of samples, grown at 383 °C, was obtained by modifying the *tert*-butanol partial pressure inside the reactor and maintaining constant the DMCd one, yielding VI/II molar ratios that ranged from 5 to 20.

HRXRD was employed to determine the epitaxial relationships between layers and substrate and to study the structural quality of the samples. All the measurements were performed in a Philips MRD x-ray diffractometer with monochromatic Cu $K\alpha_1$ radiation, which impinged on the sample after having traversed a curved graded multilayer mirror and a Ge (220) monochromator. The diffracted beam was collected by a wide open detector. Film surface morphology was monitored by SFM measurements conducted in contact mode and under ambient conditions, with a homemade microscope head[20] combined with software from Nanotec™ and a control unit Model SPM100 (Nanotec™). V-shaped Si_3N_4 sharpened cantilevers (Park Scientific Instruments) with nominal force constant of $K=0.5$ N/m and tip radius of about 20 nm were used.

III. RESULTS AND DISCUSSION

A. Crystallographic model

The in-plane orientation of CdO(110) layers on *m*-plane sapphire has been determined by measuring Φ scans on asymmetrical reflections, the azimuth Φ being defined as the angle by which the sample is rotated around an axis perpendicular to its surface (see Fig. 1). We have found the epitaxial relationships to be $[\bar{1}10]_{CdO}\|[0001]_{Sapphire}$ and $[001]_{CdO}\|[1\bar{2}10]_{Sapphire}$, confirming our previous results.[21] The directions specified by three indices refer to CdO, while a four-index notation is used to specify sapphire directions. The fact that the epitaxial relationships have been found to be independent of growth temperature and VI/II molar ratio strongly suggests that, under our experimental conditions, the substrate surface crystallographic structure controls and determines the initial nucleation. As reflected by the Φ scans

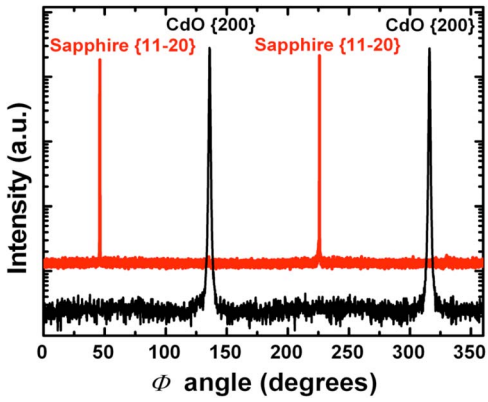

FIG. 1. (Color online) Φ scans of sapphire{$11\bar{2}0$} (displaced upwards) and CdO{200} reflections. The CdO film was grown at 290 °C with a VI/II molar ratio equal to 10.

shown in Fig. 1, CdO(110) and *m*-plane sapphire share a twofold symmetry which facilitates the bonding of cadmium and oxygen atoms across the interface.

Figure 2 is a schematic representation of the oxygen atoms, in the sapphire($10\bar{1}0$) plane, and the Cd atoms, in the CdO(110) plane, participating in the chemical bond across the substrate/layer interface. If we consider a rectangular supercell as outlined in the figure, containing one sapphire and four CdO unit cells, a reduced lattice mismatch is achieved along the directions parallel to the supercell edges: $(\Delta d/d)_{[0001]}=(4d_{[\bar{1}10]}-d_{[0001]})/d_{[0001]}=2.2\%$ and $(\Delta d/d)_{[1\bar{2}10]}=(d_{[001]}-d_{[1\bar{2}10]})/d_{[1\bar{2}10]}=-1.3\%$. From these values one would expect the CdO lattice to be under compressive stress along the $[\bar{1}10]$ direction and under a tensile stress along the [001] direction. The in-plane lattice parameters of two samples grown at different temperatures, 361 and 308 °C, were measured by recording more than 20 different reflections (see Table I). The results reveal that, although a residual tensile stress is still present in both directions, the obtained lattice parameters differ less than 0.5% from their bulk values indicating that almost complete relaxation has been achieved.

It must be pointed out that, from a fundamental point of view, the distribution of oxygen atoms in the substrate surface, as reflected by the chosen supercell, drives the orienta-

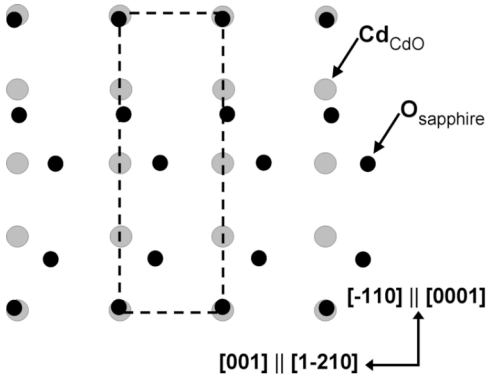

FIG. 2. (Color online) Coincident supercell (dashed line) of epitaxial CdO(110) on sapphire($10\bar{1}0$). Only Cd and O atoms belonging to CdO(110) and sapphire ($10\bar{1}0$) planes, respectively, are drawn.

TABLE I. In-plane lattice parameters along $[\bar{1}10]_{CdO}\|[0001]_{Sapphire}$ and $[001]_{CdO}\|[1\bar{2}10]_{Sapphire}$ directions for sapphire, CdO (bulk), and CdO layers grown at 361 and 308 °C with a VI/II molar ratio equal to 10.

	$d_{[\bar{1}10]\|[0001]}$ (Å)	$d_{[001]\|[1\bar{2}10]}$ (Å)
Sapphire	12.99	4.758
CdO(Bulk)	3.320	4.695
CdO(361 °C)	3.335 (4)	4.705 (5)
CdO(308 °C)	3.329 (12)	4.706 (15)

tion of the cadmium sublattice and therefore, ultimately determines the epitaxial relationships between CdO and *m*-plane sapphire. The presence of a CdO{001} axis perpendicular to the growth direction generates an anisotropic in-plane growth rate whose effects, on the morphological and structural properties of the layers, will be treated in the next sections.

B. Morphology of the CdO layers

The effect of growth temperature on the CdO surface layer morphology is illustrated in Fig. 3, where SFM topographic images of CdO layers grown at 271, 308, 344, 383, and 405 °C, as well as of a bare *m*-plane sapphire substrate are shown. At the lowest growth temperature the layer consists of grains aligned along the [001] direction with lateral dimensions of about 100×200 nm^2, the longest side being parallel to [001]. When the growth temperature is raised to 308 °C the grains coalesce and display a zigzag pattern whose periodicity is 250 nm, as deduced from both height profiles and two-dimensional self-correlation analysis of the images. As can be seen in Fig. 3(c), at a growth temperature of 344 °C the pattern is formed by ridges several microns long while the lateral periodicity remains the same. The ridges run parallel to the [001] crystallographic axis, as established from the combination of SFM images and x-ray Φ scans. However, splitting and insertion of the ridges are sometimes observed to occur (see below) thus providing deviations of an ideal one-dimensional arrangement. As the growth temperature is raised to about 383 °C the ridges become wider and the periodicity increases up to 325 nm, a process which ends by destroying the surface periodic structure at temperatures near 405 °C.

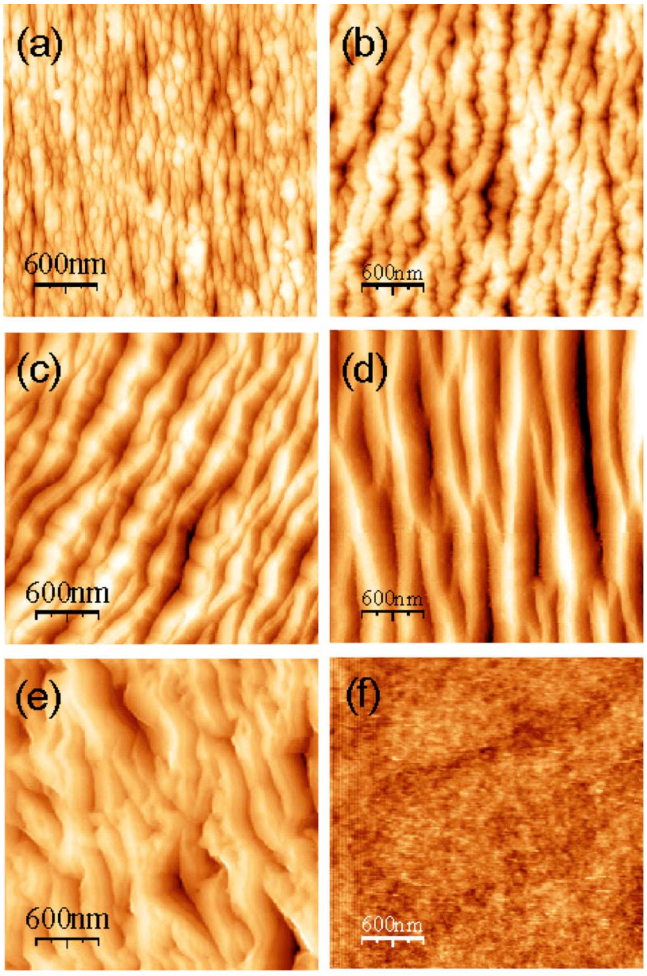

FIG. 3. (Color online) SFM topographic images (3×3 μm^2) of CdO layers grown with a VI/II molar ratio equal to 10 at different temperatures of (a) 271 °C, (b) 308 °C, (c) 344 °C, (d) 383 °C, and (e) 405 °C and of a bare *m*-plane sapphire substrate (f). The total vertical scale of the images are (a) 74 nm, (b) 130 nm, (c) 180 nm, (d) 200 nm, (e) 420 nm, and (f) 0.9 nm.

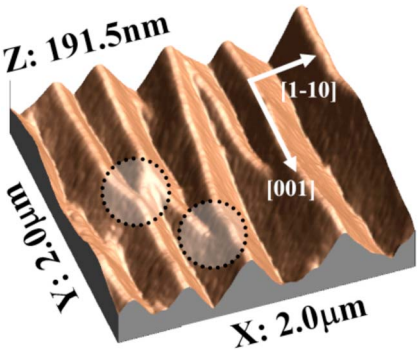

FIG. 4. (Color online) Three-dimensional representation of the SFM topographic image (2×2 μm^2) of a CdO layer grown at 383 °C with a VI/II molar ratio equal to 10. The arrows are parallel to the [001] and $[1\bar{1}0]$ directions. Morphological defects or regions of ridge intersections are enclosed by dashed circles.

Figure 4 shows a typical SFM image of a CdO surface layer obtained at 383 °C and a VI/II molar ratio of 10, where the V-groove morphology can be readily appreciated. The regularity of this ridge-and-valley structure is sometimes perturbed due to the meeting of two different wires, as marked by dashed circles in the figure. This elongated ridge-and-valley structure can be explained in terms of an enhanced growth rate along the [001] direction. Figure 5 schematically illustrates how growth can proceed on the CdO(110) atomic plane. We note that the atomic arrangement of the CdO(110)

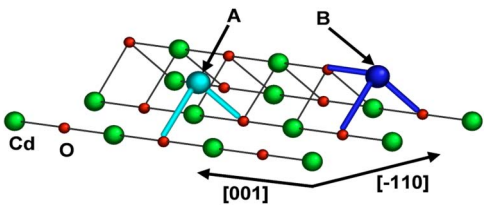

FIG. 5. (Color online) Schematic three-dimensional (3D) illustration of the growing CdO(110) layer. Positions A and B are possible sites for adatom incorporation, with wide sticks indicating the bonds formed in each case.

plane exhibits a unidirectional anisotropy, i.e., rows of either Cd or O atoms are aligned along the $[\bar{1}10]$ direction, whereas Cd and O atoms alternate along the [001] direction. Then, if a cadmium atom was incorporated at position A it would saturate two dangling bonds, and growth would take place along the $[\bar{1}10]$ direction. Alternatively, if the cadmium atom would occupy position B it would saturate three dangling bonds, one more than in position A, and it would keep on lengthening the grain parallel to the [001] axis. Thus, energetic reasons seem to be at the origin of this anisotropic in-plane growth rate which favors the development of the elongated ridge-and-valley structure observed on the grown CdO layers. The proposed mechanism is able to explain the formation of similar structures, with elongated grains parallel to the [001] direction, which had been previously encountered in the growth of other rock salt materials as NaCl (Ref. 22) and MgO.[13] Nevertheless, when the surface features are generated by processes that imply mass removal or surface reorganization, as etching or annealing, additional mechanisms must be taken into account since in these cases the rock salt materials develop structures that are elongated parallel to [001],[3,7,8,11,12] but also parallel to $[1\bar{1}0]$ (Ref. 5) or even both.[12]

To further investigate the validity of the presented model, we now discuss the possible influence of the *m*-plane sapphire substrate on the observed surface morphology. The on-axis orientation of the sapphire substrate together with the lack of a preliminary thermal annealing stage, which could have stimulated step bunching, result in an ultrasmooth surface [Fig. 3(f)] whose root-mean-square roughness is less than 0.1 nm. Therefore a possible preferential nucleation at atomic steps can be discarded and, similarly to ZnO nucleation on top of the same on-axis *m*-plane sapphire,[23] random nucleation of the first grains can be assumed. Once nucleation has taken place and if the temperature is high enough to promote surface diffusion, atoms will tend to saturate a maximum number of dangling bonds reducing the surface free energy. This energy reduction can be attained by preferential incorporation of Cd at B-type sites, which gives rise to an enhanced growth rate along [001]. At low temperatures, and hence short diffusion lengths, the atoms do not always reach the preferred incorporation sites and form separated elongated grains. An increase in growth temperature, and consequently in diffusion length, leads to grain coalescence along the [001] direction, the longest and continuous wires being achieved for temperatures between 344 and 383 °C. At still higher temperatures other competing processes take place, namely, desorption of DMCd molecules,[24] which become so important that finally control the growth process, as demonstrated by the fact that no CdO deposition could be attained at growth temperatures higher than 415 °C.

In order to analyze the influence of the surrounding atmosphere on the growing surface the morphology of the layers has been studied for varying VI/II molar ratios, while maintaining the growth temperature fixed at 383 °C. The results indicate that the ridges' lateral size, and consequently the periodicity of the pattern, remains almost constant for VI/II molar ratios between 7.5 and 12.5, while it doubles for

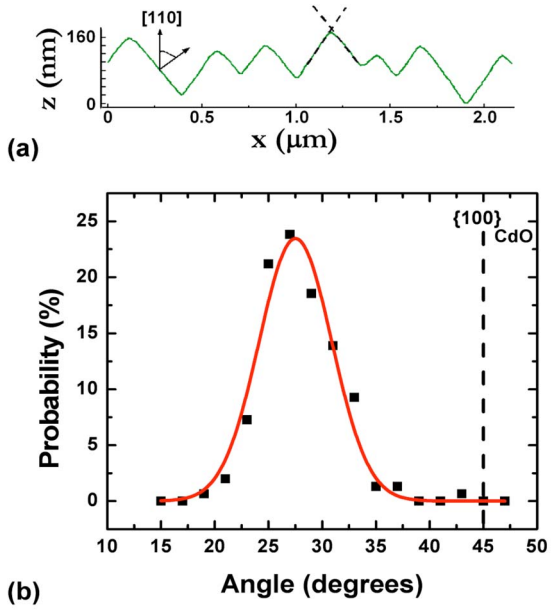

FIG. 6. (Color online) (a) Line scan along the $[1\bar{1}0]$ direction, with the angle between one of the facets and the (110) plane being indicated. (b) Distribution of measured angles between the facets exposed at the ridges and the (110) surface plane. The solid line is the data Gaussian fit.

smaller and bigger VI/II molar ratios. Obviously a quantitative description of the growth process, which would account for the detected periodicities, should consider the effects of anisotropic surface diffusion and the influence of Schwoebel barriers limiting the diffusion up and down the facets. Nevertheless, a closer observation of the CdO layer morphology leads to additional crystallographic information, including the orientation of the exposed facets. Valuable information concerning surface energy can be still obtained by evaluating the angle between the facets and the (110) plane (layer orientation).[10] Possible errors in angle estimation due to the finite size of the SFM tip[25,26] as well as errors due to any nonperpendicularity between the sample and SFM tip have been minimized by a careful measurement on the SFM images. Hence, angles have not been calculated from single facets but from pairs of facets defining a ridge [see Fig. 6(a)]. Independent measurements have been done perpendicular to each ridge, far apart from ridges intersection regions and avoiding both the valley bottom and the crest. Several hundreds of facets, corresponding to all samples but those grown at 271 and 405 °C, have been considered so that a reliable statistical counting can be assumed. The results have been plotted in Fig. 6(b) together with their Gaussian fit, following previous analysis.[11,12,27] The mean facet inclination with respect to (110) is found to be 28°, with a standard deviation of 7°.

In order to identify the morphological facets with a crystallographic plane one must bear in mind that the ridges run parallel to [001], which implies that in the (110) stereographic projection the possible crystallographic planes lie along the line connecting the (110) pole and the $(1\bar{1}0)$ and $(\bar{1}10)$ poles, that is, they must share the same [001] zone axis. Among the planes that verify this condition and restricting ourselves to Miller index as low as possible, the (310)

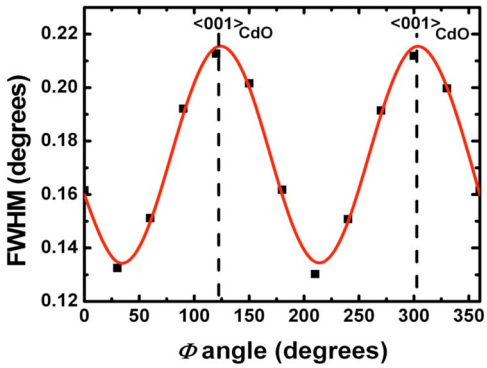

FIG. 7. (Color online) FWHM of the symmetrical CdO(220) rocking curve as a function of the azimuth angle for a sample grown at 383 °C with a VI/II molar ratio of 12.5 and the fitted sinusoidal curve. The dashed lines indicate the azimuths for which the incident beam is parallel to the CdO[001] in-plane axis.

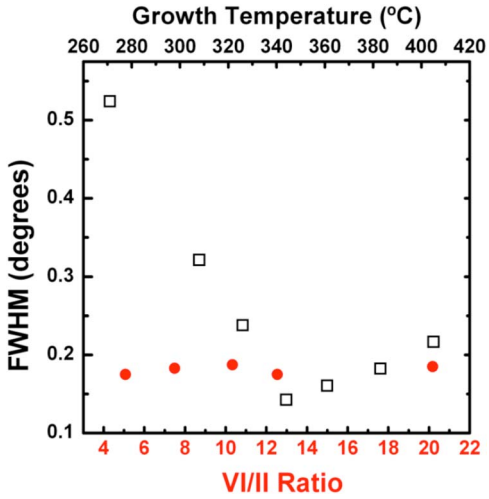

FIG. 8. (Color online) Mean FWHM of the CdO(220) rocking curve as a function of growth temperature, for layers grown with a VI/II molar ratio equal to 10 (open squares), and as a function of VI/II molar ratio, for layers grown at 383 °C (closed circles).

and (720) planes, which are inclined at 26.6° and 29.1° from CdO(110), are the closest to the measured angle. In particular, the ascription of (310) and (130) orientations to adjacent facets is plausible, since these are stepped surfaces consisting of (110) and (100) facets, i.e., the grown layer orientation and the lowest energy surface, respectively. According to theoretical calculations on MgO(110) and MgO(100) vicinal surfaces the minimum surface energy corresponds to the (100) plane,[10] which in our case would give facets forming 45° with respect to (110), as indicated by the dashed line in Fig. 6. Further work seems to be necessary to clarify this disagreement between theory and experiment, since even though some studies concerned with faceting of rock salt materials have reported {100}-type facets,[13,22] higher energy surfaces as {530} (Ref. 11) and {320} (Ref. 12) have been also detected.

C. Microstructure of the CdO layers

We have shown that some of the morphological features observed on the samples were due to an anisotropic in-plane growth rate. To analyze its influence on the microstructure and crystalline quality of the layers, the rocking curve of the symmetric (220) reflection was measured for different azimuths (Φ angles) at ΔΦ intervals of 30°. The full width at half maximum (FWHM) of the symmetric reflection, for a sample grown at 383 °C with a VI/II molar ratio of 12.5, is plotted as a function of the azimuth in Fig. 7. Minimum values of FWHM are found at 30° and 210°, i.e., 180° apart. At these azimuths, the projection of the incident beam was parallel to the $[\bar{1}10]$ direction, that is, perpendicular to the grooves' longitudinal axis. On the other hand, when the [001] in-plane direction was contained within the scattering plane the crystallographic mosaicity attained a maximum. This particular angular dependence indicates that crystal tilting is much easier along the grooves than perpendicular to them. It seems then, that the enhanced growth rate along [001] does deteriorate the crystal quality. The cause of the anisotropic broadening is still uncertain and several reasons can be invoked; among them, lateral constrains due to grain frontiers and/or an inhomogeneous distribution of crystal defects, such as screw dislocations, are fairly probable. Since an anisotropic broadening of the symmetrical rocking curve has been found a mean FWHM value, obtained by averaging values corresponding to different azimuths, has been used to compare the crystalline quality of the samples.

In Fig. 7 the fit of the FWHM experimental data to a sinusoidal curve is also depicted. It is the mean value of the fitting curve, which from now on will be referred to as the mean FWHM of the rocking curve, what has been chosen to compare the layer quality of the different samples. In Fig. 8, this mean FWHM of the (220) rocking curve has been plotted as a function of growth temperature and VI/II molar ratio. The rocking curve mean FWHM values decrease from 0.22°, at 405 °C, to the minimum attained value of 0.14° at 344 °C, which is as good as the best values previously obtained on CdO layers.[18,28] At this growth temperature the layers exhibited the longest wires, with their continuity being maintained along several microns. For lower temperatures the crystalline quality deteriorates faster, as revealed by the stepper dependence of the FWHM at the low-temperature side of the minimum. This worsening of the crystal quality corresponds to the transition from aligned wires to zigzag ripples and finally to ordered but discontinuous grains. The achievement of a minimum FWHM value at temperatures in the order of 344 °C is due to the presence of two competing processes, namely, surface diffusion and DMCd desorption, which determine the crystalline quality and which show opposite effects with increasing temperature. On the one side surface diffusion is enhanced when rising the growth temperature, resulting on the crystalline quality improvement found in the temperature range of 270–344 °C; on the other hand, a temperature increase promotes larger DMCd desorption which, in turn, favors the appearance of defects related with a Cd-deficient atmosphere. Thus, a tradeoff between enhanced surface diffusion and minimized DMCd desorption results in a minimum rocking curve mean FWHM at around 344 °C.

On the contrary the mean FWHM of the rocking curve is almost VI/II molar ratio independent, with values varying

less than 50 arc sec even for the extreme VI/II molar ratios used. The fact that the structural quality of the layers does not rely on the VI/II molar ratio but that the periodicity of the ridge-and-valley structure does, it enables to employ this growth parameter to design the topographic characteristics of the samples while maintaining a good crystalline quality. In this sense we can fix the growth temperature at 344 °C, where we obtain simultaneously the longest aligned wires and the smallest mosaicity and modify the VI/II molar ratio to act on the surface periodicity.

IV. CONCLUSIONS

CdO(110) layers have been grown on *m*-plane sapphire substrates by MOVPE. The layers consist of a ridge-and-valley structure aligned parallel to CdO[001] that, in the temperature range of 344–383 °C, gives rise to ordered and continuous wires several microns long. The inclination of the ridge facets with respect to CdO(110) has been measured to be about 28°, irrespective of the VI/II molar ratio or growth temperature employed and consistent with a (310) orientation.

A model describing the epitaxy of CdO(110) on *m*-plane sapphire has been proposed, with the orientation of the CdO lattice being determined by the oxygen distribution in the substrate surface. It has been proved that the presence of a [001] axis within the layer surface results in an anisotropic in-plane growth rate that determines the surface morphology, leading to elongated wires, and the structural properties, increasing the mosaicity parallel to [001]. It has been found that the layers exhibiting the best structural properties, in terms of rocking curve FWHM, coincide with those having the longest and well-ordered wires.

ACKNOWLEDGMENTS

This work was partially financed by the Spanish Government under Grant Nos. MAT2001-2920-C03, MAT2004-06841, and GV-Grupos 03/098, and by SOXESS European Network. Two of the authors (J.Z.-P. and C.M.) thank the Spanish MECD for their predoctoral scholarships.

[1] For a recent review in patterned surfaces see: M. Geissler and Y. Xia, Adv. Mater. (Weinheim, Ger.) **16**, 1249 (2004) and references therein.
[2] R. Nötzel, Z. Niu, M. Ramsteiner, H. P. Schönherr, A. Tranpert, L. Däweritz, and K. H. Ploog, Nature (London) **392**, 56 (1998).
[3] T. Teranishi, A. Sugawara, T. Shimizu, and M. Miyake, J. Am. Chem. Soc. **124**, 4210 (2002).
[4] A. Sugawara and M. R. Scheinfein, Phys. Rev. B **56**, R8499 (1997).
[5] S. Okamoto, O. Kitakami, T. Miyazaki, Y. Shimada, Y. K. Takahashi, and K. Hono, J. Appl. Phys. **96**, 5217 (2004).
[6] J. Fujita, H. Watanabe, Y. Ochiai, S. Manako, J. S. Tsai, and S. Matsui, Appl. Phys. Lett. **66**, 3065 (1995).
[7] A. Sugawara, Y. Haga, and O. Nittono, J. Magn. Magn. Mater. **156**, 151 (1996).
[8] A. Sugawara, T. Coyle, G. G. Hembree, and M. R. Scheinfein, Appl. Phys. Lett. **70**, 1043 (1997).
[9] V. E. Henrich, Surf. Sci. **57**, 385 (1976).
[10] J. Goniakowski and C. Noguera, Surf. Sci. **340**, 191 (1995).
[11] G. Chern, J. J. Huang, and T. C. Leung, J. Vac. Sci. Technol. A **16**, 964 (1998).
[12] D. R. Giese, F. J. Lamelas, H. A. Owen, R. Plass, and M. Gajdardziska-Josifovska, Surf. Sci. **457**, 326 (2000).
[13] A. Sugawara and K. Mae, Surf. Sci. **558**, 211 (2004).
[14] D. Wolf, Phys. Rev. Lett. **68**, 3315 (1992).
[15] D. Wolf, Solid State Ionics **75**, 3 (1995).
[16] T. Makino, Y. Segawa, M. Kawasaki, A. Ohtomo, R. Shiroki, K. Tamura, T. Yasuda, and H. Koinuma, Appl. Phys. Lett. **78**, 1237 (2001).
[17] R. J. Guerrero-Moreno and N. Takeuchi, Phys. Rev. B **66**, 205205 (2002).
[18] J. Zúñiga-Pérez, C. Munuera, C. Ocal, and V. Muñoz-Sanjosé, J. Cryst. Growth **271**, 223 (2004).
[19] R. Tena-Zaera, J. Zúñiga-Pérez, C. Martínez-Tomás, and V. Muñoz-Sanjosé, J. Cryst. Growth **264**, 237 (2004).
[20] W. F. Kolbe, D. F. Ogletree, and M. B. Salmeron, Ultramicroscopy **42–44**, 1113 (1992).
[21] J. Zúñiga-Pérez, C. Martínez-Tomás, and V. Muñoz-Sanjosé, Phys. Status Solidi C **2**, 1233 (2005).
[22] A. Sugawara and K. Mae, J. Cryst. Growth **237–239**, 201 (2002).
[23] C. Munuera, J. Zúñiga-Pérez, J. F. Rommeluere, V. Sallet, R. Triboulet, F. Soria, V. Muñoz-Sanjosé, and C. Ocal, J. Cryst. Growth **264**, 70 (2004).
[24] A. B. M. A. Ashrafi, H. Kumano, I. Suemune, Y. W. Ok, and T. Y. Seong, Appl. Phys. Lett. **79**, 470 (2001).
[25] E. Saiz, R. M. Cannon, and A. P. Tomsia, Acta Mater. **47**, 4209 (1999).
[26] U. D. Schwarz, H. Haefke, P. Reimann, and H. Gunterodt, J. Microsc. **173**, 183 (1994).
[27] J.-K. Zuo, J. M. Carpinelli, D. M. Zehner, and J. F. Wendelken, Phys. Rev. B **53**, 16013 (1996).
[28] M. Yan, M. Lane, C. R. Kannewurf, and R. P. H. Chang, Appl. Phys. Lett. **78**, 2342 (2001).